IIETA International Information and Engineering Technology Association
Advancing the World of Information and Engineering

Revue des Composites et des Matériaux Avancés-Journal of Composite and Advanced Materials
Vol. 32, No. 6, December, 2022, pp.265-269
Journal home page:http://iieta.org/journals/rcma

Investigation of the Impact of Magnesium Doping on the Structural and Dielectric Properties of the Compound: $(Na_{0.5}Bi_{0.5})_{1-x}Mg_x[(Ti_{0.8}Zr_{0.2})_{0.9}(Nb_{2/3}Zn_{1/3})_{0.1}]O_3$ (NBMTZNZ)

Ouahab Zakaria*, Bounab Karima, Necira Zoulikha

Laboratory of Applied Chemistry, Department of Science Matter, University of Biskra, BP.145, RP Biskra 07000, Algeria

Corresponding Author Email: zakaria.wahab@univ-biskra.dz

https://doi.org/10.18280/rcma.320601

Received: 29 August 2022
Accepted: 29 November 2022

Keywords:
BNT, perovskite, DRX, SEM, molten salt, dielectric

ABSTRACT

Our research is based on the production of BNT ceramics, abbreviated as NBMTZNZ. And study its structural and electrical properties. Using x-rays, electronic scanning, and non-electrical measurements, we analyzed the samples. The results obtained are of considerable value, allowing them to be exploited to develop the use of our compound.

1. INTRODUCTION

Inorganic compounds made by metals or semi-metals with non-metallic elements are called ceramics. A wide range of inorganic materials contains materials such as clay, sand and feldspar [1]. The abundance of raw materials has a lot of advantages such as: easy processing, simple manufacturing, relatively low cost and easy of use etc. Using the ceramics is increased with reasons of hardness, heat resistance [2]. Ceramics are typically produced by forming ceramic particles in to a desired shape and applying heating a process known as firing. Optimization of the forming process can require multiple rounds so forming and firing to fine-tune the forming conditions. However, conventional firing is highly energy-intensive [3, 4]. Ceramics are classified as inorganic and non-metallic materials that are essential to our daily life style. Ceramic and materials engineers are the people who design the processes in which these products can be made, create new types of ceramic products, and find different uses for ceramic products in everyday life. The properties of ceramic materials, like all materials, are dictated by the types of atoms present, the types of bonding between the atoms, and the way the atoms are packed together. This is known as the atomics cale structure. Most ceramics are made up of two or more elements. This is called a compound. For example, alumina (Al_2O_3), is a compound made up of aluminium atoms and oxygen atoms. The atoms in ceramic materials are held to gather by a chemical bond. The two most common chemical bonds for ceramic materials are covalent and ionic. For metals, the chemical bond is called them etallic bond. The bonding of atoms together is much stronger in covalent and ionic bonding than in metallic. That is why, generally speaking, metals are ductile and ceramics are brittle. Due to ceramic materials wide range of properties, they are used for a multitude of applications. In general, most ceramics are: hard, wear-resistant, brittle, refractory, the malinsulators, electrical insulators, nonmagnetic, oxidationres istant, prone to the rmalshock, and chemically stable. Ceramics have replaced metals in most of the tribological application because it has higher hardness, good thermals t ability at a higher temperature and better wear resistance etc. To improve the performance and life of the ceramics, the or etical and practical investigation of its characteristics are essential. The Tribological behavior of ceramics is a complex phenomenon on and requires added efforts to develop better understanding. The wear of material is influenced by applied load, sliding speed, surrounding temperature, time of contact, touching geometry, lubrication and its chemistry, material surface characteristics such as composition as well as roughness and the amount of oxygen present. Many works were one to study the wear characteristics of ceramics. Lead-containing ferroelectric materials such as Pb $(Zr_{1-x}Ti_x)$ O_3 (PZT) based ceramics (together with other toxic materials), have been widely used in numerous technological applications due to their excellent piezoelectric properties. However, the rapid growing amount of electronic residues and it's in correct elimination is becoming a major environmental problem. A consequence of this global issue, since 2003 the European Union included the PZT in its legislation, joint with other danger ous substances that's should be replaced with safe materials [5]. The dielectric ceramics Pb $(Zr,Ti)O_3$, abbreviated (PZT) are very sensitive oxides to insert ion or substitute ion at site A(and/or) site B, because of their simple perovskite ABO_3 structure. The purpose of doping is often related to the improvement of ceramic properties for their industrial applications (sensors, actuators and resonators) [2]. Lead-containing ferroelectric materials such as Pb (Zr, Ti) O_3(PZT) and PZT-based [6, 7]. Multi-component ceramics have been extensively utilized as sensors, actuators and ultrasonic transducers in various electronics due toits excellent piezoelectric properties. However, Problems with the vaporization of PbO during the sintering process and treatment of Pb-containing products cause critical environmental pollution. Recently, much greater consideration has been given to the study of lead-free piezoelectric materials for the replacement of lead-containing ferroelectrics [6, 7]. $Bi_{0.5}Na_{0.5}TiO_3$(BNT)-based as typical RFEs materials have recently gained a lot of attention because of their huge

Pmax(>40C/cm^2) and high Curie temperature (T_c320°C) [8]. Some success full strategies, such as A/B site doping and concurrent substitution of A and Bsites, have been proven to improve the quality of BNT-based ceramics [9, 10]. $Bi_{0.5}Na_{0.5}TiO_3$(BNT) is a ferroelectric with Bi^{3+} and Na^+ occupy the A site in the perovskite phase [11, 12]. The $Na_{0.5}Bi_{0.5}TiO_3$(NBT) and NBT based system with ABO_3 (where A=mono or divalent ions, B=tri, tetra or pentavalent ions) [13,14]. Perovskite structure is one of the principal lead-free materials [15, 16]. This work concentrates on material derived from BNT and exempted lead. The goal of this work is to synthesize the solution NBMTZNZ. We analyze the structural and dielectric characterization of these doped BNT materials. We synthesized the solid solution NBMTZNZ (such as x=0,0.02). We will try to determine the impact of variation in the value of x (which is primarily connected to the amount of magnesium in our ceramics) on the structural and dielectric properties.

2. EXPERIMENTAL PROCEDURE

2.1 Samples preparation

The ceramics $(Na_{0,5}Bi_{0,5})$ $[(Ti_{0.8}Zr_{0.2})_{0,9}(Zn_{1/3}Nb_{2/3})_{0,1}]$ O_3 and $(Na_{0,5}Bi_{0,5})_{0,98}Mg_{0,02}[(Ti_{0.8}$ $Zr_{0.2})_{0.9}(Zn_{1/3}$ $Nb_{2/3})_{0.1}]$ O_3 are prepared by molten salt method (MS). Reagent-grade Bi_2O_3 (99.0%), Na_2CO_3 (99 ,5%), TiO_2 (99,0%), ZrO_2(99,0%), ZnO (99,5%), Nb_2O_5 (99,99%) and MgO (99,0%) were weighted according to the stoichiometric ratio and mixed together at the same weight (NaCl/KCl) (1/1). Then, the mixture was crushed in a mortar of a glass for 3 hours and calcined at 900°C for 4 hours with a heating rate of 2°C/min to assure that remaining salts were removed. The goal of regrinding is to minimize agglomerates created during the calcination process, homogenize the powder, and boost its reactivity. After regrinding, the powder is compacted into pellets with a mass of 1,5 g and a diameter of around 13 mm. Natural sintering under air is used to sinter our ceramics in an alumina crucible at 1150°C. Temperature increases to the defined temperature with a speed of 2°C/min. Then, it stabilizes for 4-hour. Finally, it decreases to ambient.

2.2 Material characterization

The spectra of our sintered ceramics are created at room temperature using a vertical diffractometer «BRUKER-AXE type D8» located in the University of Biskra's X-ray laboratory. The line profiles were measured using an automatic point-by-point counting system with a 0.02° pitch. All diffraction diagrams are recorded in the angular domain $0° < 2 < 80°$, which may be sufficient for the identification of the different phases. We note that we used X'Pert HighScore for the analyzing and indexing the different lines. The micrographs of our samples are performed using a scanning electron microscope of type JEOL JSM-6390lv provided the X-ray laboratory of the University of Biskra. An operating system allows a computer to regulate it. The goal of these micrographs is to study the morphology of our samples. The density of sintered pellets is determined by geometric measurements (diameter and thickness) on each sintered pellet, with the use of a slide palmer. The formula for calculating the density (d) is as follows: $d=m / \pi(\theta/2)^2 e$. Such as: **m**: Mass of the pellet (g), **θ**: and **e**: Using an LCR meter, the dielectric permittivity and loss tangent of sintered samples were determined as a function of frequency at different temperatures (300 °K to 500 °K).

3. RESULTS AND DISCUSSION

3.1 DRX

X-ray analysis (Figure1) reveals that the pellet in the synthesis method and crystallinity in the cubic system with space group Pm-3m have the perovskite structure of (ICSD:(01-089-3109) [8, 9]. The lattice parameters were calculated from the XRD data using the cellref program as shown in Table 1.

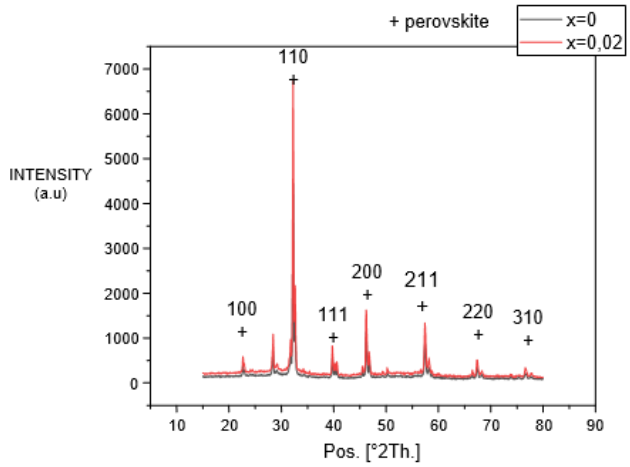

Figure 1. X-raydiffractogrammes

Table 1. Lattice parameters

Parameters	X	
	0	**0,02**
a(Å)	3.8822	3.9130
b(Å)	3.8822	3.9130
c(Å)	3.8822	3.9130
α	90°	90
β	90°	90
γ	90°	90
Grainsseize(µm)	4,806	4,695

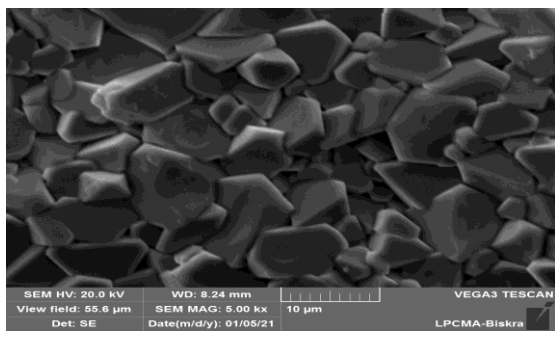

Figure 2. SEM micrograph of $(Na_{0.5}Bi_{0.5})[(Ti_{0.8}Zr_{0.2})_{0.9}(Nb_{2/3}Zn_{1/3})_{0,1}]O_3$

3.2 SEM micrograph

Figures 2 and 3 displays scanning electron microscope (SEM) photographs of compositions doped with Mg at 1150°C

sintering temperature. At first glance, the samples appear homogeneous. We suggested that the ceramic is dense and the porosity is low [8, 10]. With an increase in composition from 4.806µm for X = 0 to 4.695µm for X = 0.02, the average grain size drops as shown in Table 1. We can say that the molten salt method is suitable for synthesis our material.

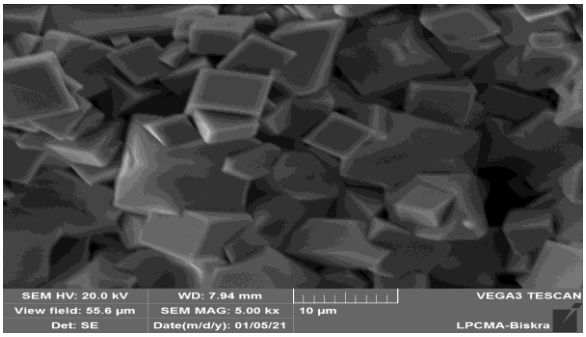

Figure 3. SEM micrographs of $(Na_{0.5}\,Bi_{0.5})_{0,98}\,Mg_{0,02}\,[(Ti_{0.8}\,Zr_{0.2})_{0.9}\,(Nb_{2/3}Zn_{1/3})_{0,1}]O_3$

3.3 Dielectric characterization

The electrical qualities of ceramic samples are related to the dielectric properties: permittivity (ε_r), Resistivity (ρ), Loss tangent (tan δ) and dielectric rigidity [11, 12]. In our work, we concentrated on determining the dielectric constant values and loss tangent values as shown in Figures 4, 5, 6, and 7. It is observed from ε_r vs T plots that ε_r increases with increasing temperature up to certain temperature and shows broad dielectric maxima around a particular temperature, represented as T_m, and it decreases slowly with temperature above T_m. It can be seen that T_m depends on the composition (x), such as T_m=400 for x=0 and 425 for x=0.02 [13]. The curves ε_r(T) exhibit the same beauty, that is, they rise with temperature, reach a maximum, then fall. One can see that the maximum electrical permittivity ε_m values for each composition (x=0 and x=0.02) are noted at 100Hz. As frequency decreases, ε_r increases until it nearly disappears at the highest frequency (100KHz) for two compositions. It has been noticed that the dielectric constant decreases as frequency increases, which can be attributed to the presence of various types of decreasing polarization [14]. The dielectric constant has frequency dependence especially, at the low frequencies(100Hz), which is called the low frequency dielectric dispersion. A strong low-frequency dielectric dispersion has also been observed in NBT which was previously reported [7, 15]. The maximum dielectric constant temperature (T_m) is related to the ferroelectric-paraelectric phase transition temperature. With the increase of frequency, the ε_m values of all samples gradually decrease, which may be ascribed to the fact that the dipole cannot be consistent with the frequency of the electric field. The Tm values move to a high temperature, showing the characteristics of frequency dispersion [16, 17]. This observation indicates a relaxation process which can be related to ferroelectric antiferroelectric phase transition [18, 19]. The factor of dissipation is connected to a rate of electrical energy loss, frequently manifested as dissipated heat [20]. Because the samples had been changed into a paraelectric phase, there was a quick reduction in the electrical loss Tanδ, which in turn reduced the polarization loss. For all samples, T_m moves toward a higher temperature as the frequency increases, indicating the presence of relaxing characteristics [21]. This increase in tanδ may be due to an increase in the electrical conduction of the residual current and absorption current [22, 23]. This increase in tanδ may be due to an increase in the electrical conduction of the residual current and absorption current [24, 25].

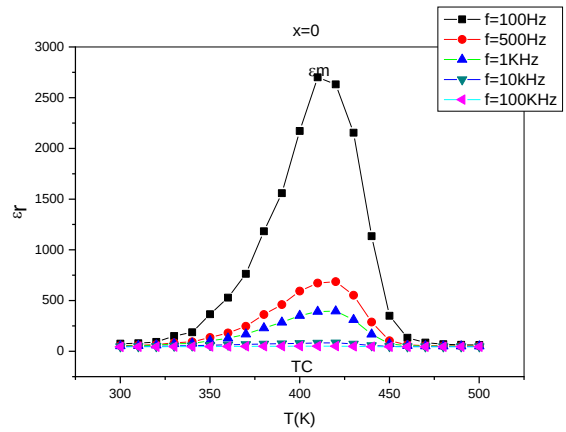

Figure 4. Dielectric constant of $Na_{0.5}\,Bi_{0.5})\,[(Ti_{0.8}\,Zr_{0.2})_{0.9}\,(Nb_{2/3}Zn_{1/3})_{0,1}]\,O_3$

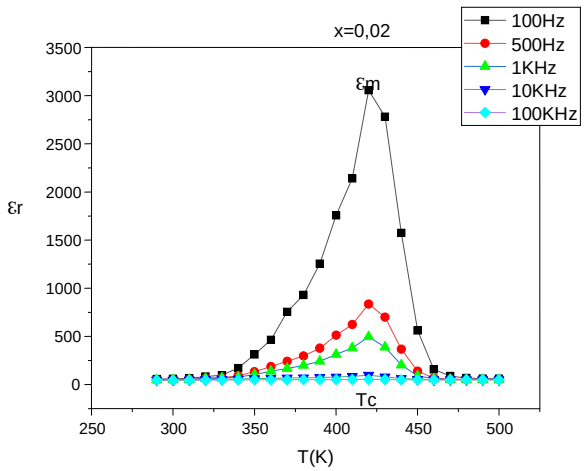

Figure 5. The dielectric constant of $(Na_{0.5}\,Bi_{0.5})_{\,0,98}\,Mg_{\,0,02}\,[(Ti_{0.8}\,Zr_{0.2})_{0.9}\,(Nb_{2/3}Zn_{1/3})_{0,1}]\,O_3$

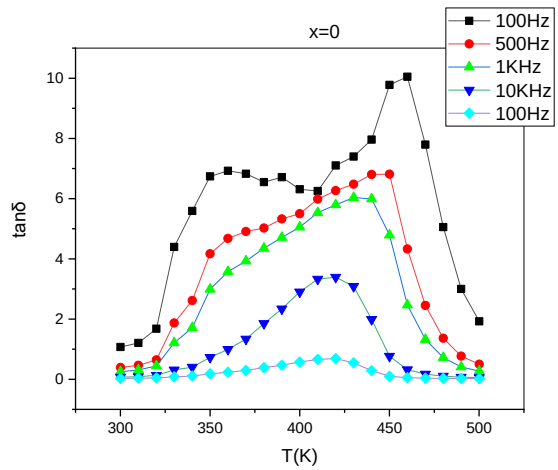

Figure 6. Loss tangent of $(Na_{0.5}Bi_{0.5})_{0,98}\,[(Ti_{0.8}Zr_{0.2})_{0.9}\,(Nb_{2/3}Zn_{1/3})_{0,1}]\,O_3$ tangent of $Na_{0.5}Bi_{0.5})\,[(Ti_{0.8}Zr_{0.2})_{0.9}\,(Nb_{2/3}Zn_{1/3})_{0,1}]\,O_3$

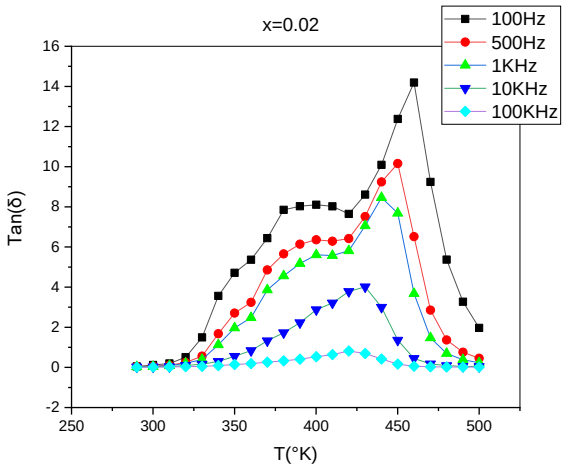

Figure 7. Loss tangent of $(Na_{0.5}Bi_{0.5})_{0,98}Mg_{0,02}[(Ti_{0.8}Zr_{0.2})_{0.9}(Nb_{2/3}Zn_{1/3})_{0,1}]O_3$

4. CONCLUSIONS

The lead free **NBMTZNZ** ceramics were prepared by using the molten salt synthesis route (MS). The effect of sintering temperature on structural and dielectric properties was investigated. The ceramics were calcined at 900°C and sintered at 1150°C. X-ray diffraction (XRD) analysis reveals that the **NBMTZNZ** ceramics have a perovskite structure, but phase pyrochlore is obtained. The morphological study by SEM analysis confirms that the samples have a relatively dense pure. The results of DRX and SEM confirmed suitability of MS. The dielectric measurements support our findings that a change in Mg values has an impact on the quality of the ceramic that we tested. We noted ε_m is 2650 for x=0 and 3000 for x=0.02 such as T_C is 400°C for x=0 and 425°C for x=0.02. All results considered a hard-ferroelectric material, can be used at law frequencies in several technological fields.

ACKNOWLEDGMENT

These studies were carried out using the equipment of the laboratory of Applied Chemistry at university of Biskra and the laboratory of engineers physicsat the university of Tiaret.

REFERENCES

[1] Akgun, O. (2020). Spectral and statistical analysis for damage detection in ceramic materials. Traitement du Signal, 37(1): 9-16. https://doi.org/10.18280/ts.370102

[2] Elsen, S.R., Ramesh, T. (2016). Analysis and optimization of dry sliding wear characteristics of zirconia reinforced alumina composites formed by conventional sintering using response surface method. Int. Journal of Refractory Metals and Hard Materials, 58: 92-103. https://doi.org/10.1016/j.ijrmhm.2016.04.007

[3] Toyokura, S. (2021). Contactless mapping of ceramic green density using optical coherence tomography. Open Ceramics, 5: 100061. https://doi.org/10.1016/j.oceram.2021.100061

[4] Ibn-Mohammed, T., Randall, C.A., Mustapha, K.B., Guo, J., Walker, J., Berbano, S., Koh, S.C.L., Wang, D., Sinclair, D.C., Reaney, I.M. (2019). Decarbonising ceramic manufacturing: A techno-economic analysis of energy efficient sintering technologies in the functional materials sector. J. Eur. Ceram. Soc., 39(16): 5213-5235. https://doi.org/10.1016/j.jeurceramsoc.2019.08.011

[5] Aurivillius, B. (1950). Mixed bismuth oxides with layer lattices III. Structure of Ba $Bi_4Ti_3O_{12}$. Arkiv Kemi., 2: 519-527.

[6] Shukla, A., Choudhary, R.N.P. (2011). High temperature Impedance and Modulus spectroscopy Characterization of La^{+3} /Mn^{+4} Modified $PbTiO_3$ Nano ceramics. Physica B: Condensed Matter., 406(13): 2492-2500. https://doi.org/10.1016/j.physb.2011.03.030

[7] Sambasiva Rao, K., Tilak, B., Varada Rajulu, K.C., Swathi, A., Haileeyesus, W. (2011). Electrical properties of barium and zirconium modified NBT ferroelectric ceramics. AIP Conf Proc., 1372: 29-33. https://doi.org/10.1063/1.3644413

[8] Acharya, S.K., Lee, S.K., Hyung, J.H., Yang, Y.H., Kim, B.K., Ahn, B.G. (2012). Ferroelectric and piezoelectric properties of lead-free $BaTiO_3$ doped $Bi_{0.5}Na_{0.5}TiO_3$ thin films from metal-organic solution deposition. J. Alloys Compd., 540: 204-209. https://doi.org/10.1016/j.jallcom.2012.06.071

[9] Scarisoreanu, N., Craciun, F., Ion, V., Birjega, S., Dinescu, M. (2007). Structural and electrical characterization of lead-free ferroelectric $Na_{1/2}Bi_{1/2}TiO_3$–$BaTiO_3$ thin films obtained by PLD and RF-PLD. Appl. Surf. Sci., 254(4): 1292-1297. https://doi.org/10.1016/j.apsusc.2007.09.036

[10] Hao, H., Liu, H., Liu, Y., Cao, M., Ouyang, S. (2007). Lead-free $SrBi_4Ti_4O_{15}$ and $Bi_4Ti_3O_{12}$ material fabrication using the microwave-assisted molten salt synthesis method. J. Am. Ceram. Soc., 90(5): 1659-1662. https://doi.org/10.1111/j.1551-2916.2007.01632.x

[11] Wisedsri, R., Chaisuwan, T., Wongkasemjit, S. (2013). Simple route to bismuth titanate from bismuth glycolate precursor via sol–gel process. Materials Research Innovations, 17(1): 43-48. https://doi.org/10.1179/1433075X12Y.0000000003

[12] Li, Y., Chen, W., Zhou, J., Xu, Q., Sun, H., Xu, R. (2004). Dielectric and piezoelectric properties of lead free $(Na_{0.5}Bi_{0.5})$ TiO_3–Na NbO_3 ceramics. Materials Science and Engineering: B, 112(1): 5-9. https://doi.org/10.1016/j.mseb.2004.04.019

[13] Pal, V., Dwivedi, R.K., Thakur, O.P. (2014). Synthesis and ferroelectric behavior of Gd doped BNT ceramics. Current Applied Physics, 14(1): 99-107. https://doi.org/10.1016/j.cap.2013.10.007

[14] Yang, F., Pan, Z., Ling, Z., Hu, D., Ding, J., Li, P. (2021). Realizing high comprehensive energy storage performances of BNT-based ceramics for application in pulse power capacitors. Journal of the European Ceramic Society, 41(4): 2548-2558. https://doi.org/10.1016/j.jeurceramsoc.2020.11.049

[15] Oh, T. (2006). Dielectric relaxor properties in the system of $(Na1-xKx)_{1/2}Bi_{1/2}TiO_3$ ceramics. Japanese Journal of Applied Physics, 45(6R): 5138-5138. https://doi.org/10.1143/JJAP.45.5138

[16] Ramana, E.V., Bahuguna Saradhi, B.V., Suryanarayana, S.V., Sankaram, T.B. (2005). Synthesis and characterisation of 1-x $(Na_{1/2}Bi_{1/2}TiO_3)$-x $(BiFeO_3)$ ceramics. Ferroelectrics, 324(1): 55-61. https://doi.org/10.1080/00150190500323693

[17] Yu, Z., Liu, Y., Shen, M., Qian, H., Li, F., Lyu, Y. (2017). Enhanced energy storage properties of $BiAlO_3$ modified $Bi_{0.5}Na_{0.5}TiO_3$–$Bi_{0.5}K_{0.5}TiO_3$ lead-free antiferroelectric ceramics. Ceramics International, 43(10): 7653-7659. https://doi.org/10.1016/j.ceramint.2017.03.062

[18] Li, L., Hao, J., Xu, Z., Li, W., Chu, R. (2018). Electric field-induced large strain in Ni/Sb-co doped ($Bi_{0.5}Na_{0.5}$) TiO_3-based lead-free ceramics. Journal of Electronic Materials, 47(2): 1512-1518. https://doi.org/10.1007/s11664-017-5935-5

[19] Silva Jr, P.S., Diaz, J.C.C.A., Florêncio, O., Venet, M., M'Peko, J.C. (2016). Analysis of the phase transitions in BNT-BT lead-free ceramics around morphotropic phase boundary by mechanical and dielectric spectroscopies. Archives of Metallurgy and Materials, 61(1): 17-20. https://doi.org/10.1515/amm-2016-0008

[20] Hadjadj, S., Boutarfaia, A., Zenkhri, L., Durga, C.S.S., Ruben, N., Chen, F. (2019). Structural and dielectric study of a PLNZNT ceramic material doped with chromium. Annales de Chimie: Science des Materiaux, 43(2): 69-74. https://doi.org/10.18280/acsm.430201

[21] Zeng, M., Liu, J., Li, H. (2021). Structural and dielectric properties of (1-x)($Sr_{0.7}Pb_{0.15}Bi_{0.1}$)$TiO_{3-x}$($Bi_{0.5}Na_{0.5}$)$TiO_3$ energy storage ceramic capacitors. Journal of Alloys and Compounds, 861: 158535. https://doi.org/10.1016/j.jallcom.2020.158535

[22] Menasra, H., Necira, Z., Bounabe, K., Abba, M., Meklid, A., Boutarfaia, A. (2018). Structural and electrical characterization of La substituted PMS-PZT (Zr/Ti: 60/40) ceramics. Materials Science-Poland, 36(1): 1-6. https://doi.org/10.1515/msp-2018 0033

[23] Tareev, B. (1979). Physics of Dielectric Materials. Mir Publisher, Moscow, 157-157.

[24] Mohammed, A.S.K., Kurovics, E., Ibrahim, J.F.M., Tihtih, M., Simon, A., Géber, R. (2022). Revue des Composites et des Matériaux Avancés-Journal of Composite and Advanced Materials, 32(5): 223-228, https://doi.org/10.18280/rcma.320502

[25] Hayder, N., Hashim, A., Habeeb, M.A., Rabee, B.H., Hadi, A.G., Mohammed, M.K. (2022). Revue des Composites et des Matériaux Avancés-Journal of Composite and Advanced Materials, 32(5): 261-264. https://doi.org/10.18280/rcma.320507

NOMENCLATURE

a,b,c	Lattice parameters in Å
D	Density (g/cm^3)
e	Pellet thickness (cm)
M	pellet Masse (g)
T_c	Curie temperature (℃)
T_m	Maximum temperature (℃)

Greeks ymbols

α,β,γ	Mesh angls(°)
Θ	Pellet diameter(cm)
π	3,14

Subscripts

BNT	$Bi_{0.5}Na_{0.5}TiO_3$
DRX	X-ray diffractogrammes
MS	Molten salt method
SEM	Scaning elcetronic microscop
NBMTZNZ	$(Na_{0.5}Bi_{0.5})_{1-x}Mg_x[(Ti_{0.8}Zr_{0.2})_{0.9}(Nb_{2/3}Zn_{1/3})_{0.1}]O_3$